

Revision 1

**Joegoldsteinite: A new sulfide mineral (MnCr₂S₄) from the IVA iron meteorite,
Social Circle**

Junko Isa^{1*}, Chi Ma^{2*} and Alan E. Rubin^{1,3}

¹Department of Earth, Planetary, and Space Sciences, University of California, Los Angeles,
California 90095-1567, USA

²Division of Geological and Planetary Sciences, California Institute of Technology, Pasadena,
California 91125, USA

³Institute of Geophysics and Planetary Physics, University of California, Los Angeles,
California 90095-1567, USA

*e-mail: jisa@ucla.edu; chi@gps.caltech.edu; aerubin@ucla.edu

ABSTRACT

Joegoldsteinite, a new sulfide mineral of endmember formula MnCr₂S₄, was discovered in the Social Circle IVA iron meteorite. It is a thiospinel, the Mn analogue of daubréelite (Fe²⁺Cr₂S₄), and a new member of the linnaeite group. Tiny grains of joegoldsteinite were also identified in the Indarch EH4 enstatite chondrite. The chemical composition of the Social Circle sample by electron microprobe is (wt%) S 44.3, Cr 36.2, Mn 15.8, Fe 4.5, Ni 0.09, Cu 0.08, total 101.0, giving rise to an empirical formula of (Mn_{0.82}Fe_{0.23})Cr_{1.99}S_{3.95}. The crystal structure, determined by electron backscattered diffraction, is a *Fd3m* spinel-type structure with $a = \text{\AA}$, $V = 1033.4 \text{\AA}^3$, and $Z = 8$.

Keywords: Joegoldsteinite, MnCr₂S₄, new sulfide mineral, thiospinel, Social Circle IVA iron meteorite, Indarch EH4 enstatite chondrite

INTRODUCTION

30 Thiospinels have a general formula of AB_2X_4 where A is a divalent metal, B is a
31 trivalent metal and X is a -2 anion, typically S, but in some cases Se or Te. Some
32 thiospinels are magnetic semiconductors and have been studied extensively by materials
33 scientists. Synthetic $MnCr_2S_4$ is known to be a ferrimagnetic insulator (Menyuk et al. 1965;
34 Darcy et al. 1968; Lotgering 1968; Plumier 1980; Denis et al. 1970) and recent single crystal
35 measurements have documented two different anomalies in heat capacity that correlate with
36 magnetic phase transformations (Tsurkan et al. 2003). The complex behavior of thiospinel
37 magnetism results from ferrimagnetic ordering of the Cr and Fe sublattices (Bertinshaw et al.
38 2014).

39 Joegoldsteinite is the first known natural occurrence of $MnCr_2S_4$. It is present as two
40 13-15- μ m-size subhedral inclusions in the Social Circle IVA iron meteorite. The meteorite
41 itself was found as a single ~100-kg mass in Georgia, USA in 1926 during ploughing
42 (Buchwald 1975).

43 The IVA irons constitute the third largest “magmatic” iron-meteorite group; each
44 magmatic group is modeled as having formed by fractional crystallization in the metallic core
45 of a differentiated asteroid (e.g., Scott et al. 1996). IVA iron meteorites are fine octahedrites
46 showing Widmanstätten patterns (Buchwald 1975). The bulk Ni concentrations range from
47 ~60 to ~120 mg/g. Studies of the metallographic cooling rates in IVA iron meteorites have
48 been controversial for several decades (e.g., Willis and Wasson, 1978a,b; Moren and

49 Goldstein, 1978). Relative to other magmatic irons, the IVA group has large depletions in S,
50 Ga and Ge (Wasson and Richardson 2001). The Ir-rich IVA samples are characterized by
51 lower bulk Ir/Au ratios than comparable members of other iron-meteorite groups (Wasson
52 and Richardson 2001).

53 The Mn-Cr thiospinel, joegoldsteinite, was approved as a new mineral by the
54 International Mineralogical Association (IMA) in August 2015. It was named in honor of
55 Joseph (Joe) I. Goldstein (1939-2015), Distinguished Professor emeritus of mechanical and
56 industrial engineering and former dean of the College of Engineering at the University of
57 Massachusetts, Amherst. Before arriving at Amherst, Goldstein was the T. L. Diamond
58 Distinguished Professor of Metallurgy and R. D. Stout Professor of Materials Science and
59 Engineering at Lehigh University; he served as vice president for graduate studies and
60 research and as director of Lehigh's Electron Optical Laboratory. Goldstein was well
61 known for his fundamental contributions to research on iron meteorites, metallographic
62 cooling rates, Fe-Ni phase equilibria, electron microscopy and microanalysis.

63

64 **SAMPLES AND ANALYTICAL METHODS**

65 A polished thick section of Social Circle (TK 724) was made from a 2×3×5-mm-size
66 aliquot from the UCLA meteorite collection. It was examined in reflected light with an
67 Olympus BX60 petrographic microscope and by backscattered-electron (BSE) imaging using

68 a VEGA Tescan SEM at UCLA and a Zeiss 1550VP field-emission SEM at Caltech. Phases
69 were analyzed by energy-dispersive X-ray spectroscopy (EDX) with the SEM and by a JEOL
70 8200 electron microprobe (EPMA) (WDS mode, 15 kV, 15 nA, focused beam mode using
71 ZAF corrections) at UCLA. The chemical composition is shown in Table 1. A synthesized
72 FeCr_2S_4 single crystal, grown by a chemical transport reaction method similar to that of
73 Tsurkan et al. (2001), was used as a standard for S, Cr and Fe measurements.

74 Single-crystal electron backscatter diffraction (EBSD) analyses at a sub-micrometer
75 scale using methods described in Ma and Rossman (2008, 2009) were performed using an
76 HKL EBSD system on the Zeiss 1550VP SEM at Caltech, operated at 20 kV and 6 nA in
77 focused-beam mode with a 70° tilted stage and in a variable-pressure mode (20 Pa). The
78 EBSD system was calibrated using a single-crystal silicon standard. The structure was
79 determined and cell constants were obtained by matching the experimental EBSD patterns
80 with structures of synthetic MnCr_2S_4 and daubr elite.

81

82 **RESULTS**

83 **Petrography and mineral chemistry**

84 Joegoldsteinite occurs as two subhedral inclusions, 13 μm and 15 μm in diameter, in
85 Social Circle thick section TK 724 (Fig. 1). Physical properties were not measured because
86 of the small grain size; however, they are likely to be close to those of daubr elite. Optical

87 properties of joegoldsteinite were assessed in reflected light and compared to daubréelite
88 grains that are adjacent to metallic Fe-Ni in the Aliskerovo and NWA 4704 IIIIE iron
89 meteorites (e.g., Breen et al. 2015). Both minerals have similar reflectivity and color.
90 More accurate comparisons could be made if a single section were available that contained
91 grains of both phases. Electron microprobe data indicate that the empirical formula (based
92 on 7 atoms) is $(\text{Mn}_{0.82}\text{Fe}_{0.23})\text{Cr}_{1.99}\text{S}_{3.95}$; the general formula is $(\text{Mn,Fe})\text{Cr}_2\text{S}_4$ and the
93 end-member formula is MnCr_2S_4 . The calculated density, based on the empirical formula, is
94 3.71 g cm^{-3} .

95 Joegoldsteinite is a thiospinel, the Mn analogue of daubréelite ($\text{Fe}^{2+}\text{Cr}_2\text{S}_4$), and a new
96 member of the linnaeite group. In joegoldsteinite and daubréelite, Fe and Mn probably have
97 a +2 valence and occupy the tetrahedral (A) sites. Chromium may have a +3 valence and
98 occupy the octahedral (B) sites. Because joegoldsteinite is Fd3m spinel type, we do not
99 think there is S-S bonding in the structure (a requirement if Cr were +2; McCoy et al., 2014).
100 It thus seems likely that Cr in both daubréelite and joegoldsteinite is located in the octahedral
101 site; Cr³⁺ should thus be thermodynamically stable at a sufficiently high sulfur fugacity. It
102 seems reasonable that enstatite chondrites could contain both Cr³⁺ and Cr²⁺ in different
103 minerals. (Along with nearly pure forsterite and enstatite, some E3 chondrites contain
104 oxidized mafic silicates, i.e., moderately ferroan olivine (Fa₁₁) and low-Ca pyroxene (Fs₁₈)
105 grains; Weisberg and Kimura 2012).

106 Some tiny grains of joegoldsteinite associated with troilite (FeS) and niningerite
107 ((Mg,Fe)S) were also observed in the Indarch EH4 enstatite chondrite (Fig. 2), but the grains
108 are too small for accurate quantitative analysis by EPMA.

109

110 **Crystal structure**

111 The EBSD patterns match the cubic space group *Fd3m* spinel-type structure ($a =$
112 10.11 , $V = 1033.4 \text{ \AA}^3$, $Z = 8$) and give a best fit using the MnCr_2S_4 structure from Raccach et al.
113 (1966) (Fig. 3), with a mean angular deviation of 0.40° to 0.45° . The cell parameters are
114 taken from data for the matching phase in Raccach et al. (1966). X-ray powder diffraction
115 data (Table 2, in \AA for $\text{CuK}\alpha_1$, Bragg-Brentano geometry) were calculated from the cell
116 parameters of Raccach et al. (1966) with the empirical formula, using Powder Cell version 2.4.

117

118 **DISCUSSION**

119 **Other Mn- and Cr-bearing phases in irons and reduced meteorites**

120 The only known phases with detectable Mn in IVA irons besides joegoldsteinite are
121 daubréelite (~ 0.2 - 0.8 wt.% Mn) in Maria da Fé (this study) and orthopyroxene (~ 0.5 - 0.6
122 wt.% MnO) and clinopyroxene (~ 0.5 wt.% MnO) in Steinbach and São João Nepomuceno
123 (Scott et al. 1996).

124 Social Circle contains a few Cr-rich phases in addition to joegoldsteinite; these

125 include daubréelite (FeCr_2S_4), chromite (FeCr_2O_4), and possibly, brezinaite (Cr_3S_4)
126 (Buchwald 1975). Additional Cr-rich phases reported in magmatic iron meteorites (but not
127 in the IVA group) include carlsbergite (CrN) in several IIIAB samples and kosmochlor
128 ($\text{NaCrSi}_2\text{O}_6$) in a few IIA samples (Buchwald 1975).

129 Enstatite chondrites, such as EH4 Indarch (in which small grains of joegoldsteinite
130 were found), formed under low f_{O_2} conditions. These rocks contain mafic silicates
131 (predominantly enstatite, with minor forsterite in unequilibrated samples) with very low FeO,
132 Si-bearing metallic Fe-Ni, and sulfide phases containing cations (e.g., Na, Mg, K, Ca, Ti, Cr,
133 Mn, Fe) that partition mainly into silicates and oxides in more-oxidized assemblages (e.g.,
134 Keil 1968; Rubin and Keil 1983; Wasson et al. 1994). For example, sulfide in ordinary
135 chondrites (OC), meteorites that are much more oxidized than enstatite chondrites, is Mn free
136 (e.g., Williams et al. 1985; Rubin et al. 2002); Mn in OC occurs principally in olivine, low-Ca
137 pyroxene, Ca-pyroxene and chondrule mesostasis (e.g., Brearley and Jones 1998).

138 Additional Mn-bearing sulfides in enstatite chondrites (and related impact-melt rocks
139 and impact-melt breccias) include daubréelite (with 0.7-4.0 wt.% Mn), troilite (FeS :
140 0.02-0.39 wt.% Mn), oldhamite (CaS : 0.18-1.3 wt.% Mn), niningerite ($(\text{Mg,Fe})\text{S}$: 6.1-12.9
141 wt.% Mn), keilite ($(\text{Fe,Mg})\text{S}$: 3.4-23.7 wt.% Mn), rudashevskyite ($(\text{Fe,Zn})\text{S}$: 1.6-3.6 wt.%
142 Mn), buseckite ($(\text{Fe,Zn,Mn})\text{S}$, ~10 wt.% Mn), browneite (MnS , ~62 wt.% Mn) and
143 pentlandite ($(\text{Fe,Ni})_9\text{S}_8$: 0.66-1.1 wt.% Mn) (Keil 1968, 2007; Lin et al. 1991; Britvin et al.

144 2008; Ma et al. 2012a,b).

145

146 **Shock effects**

147 The presence of Neumann lines in Social Circle kamacite indicates that the sample
148 was shocked to at least 10 kb after cooling (Buchwald 1975). A later shock event caused
149 widespread heating of the meteorite: (a) kamacite throughout the mass recrystallized,
150 partially obliterating the Neumann lines (and forming “parallel ghost-lines”), (b) taenite and
151 plessite fields partly decomposed and underwent minor spheroidization, and (c) troilite-metal
152 eutectic shock melts formed (Buchwald 1975). It seems plausible that impact melting of the
153 sulfide assemblages increased the Mn concentration in portions of the S-rich melts,
154 facilitating the crystallization of joegoldsteinite.

155 After the formation of joegoldsteinite in Social Circle, a minor shock event caused
156 shearing in the grain in the top image of Fig. 1. Displacement by $\sim 0.2 \mu\text{m}$ occurred along a
157 kamacite grain boundary (also probably produced by shearing) running diagonally from SW
158 to NE-ENE.

159

160 **Implications**

161 It has been shown that MnCr_2S_4 can transform from the spinel structure (where
162 two-thirds of the cations are octahedrally coordinated) to the defect NiAs structure (where all

163 cations are octahedrally coordinated) at temperatures of 1000°C and pressures of 65 kb (6.5
164 GPa) (Bouchard 1967). The high-pressure structure is reversible (Vaquero et al. 2001).
165 Because of this structural reversibility, empirical observations of thiospinel minerals are
166 unlikely to be useful for constraining the formation temperatures and pressures of asteroidal
167 materials. Nevertheless, chalcospinel, thiospinel and selenospinel have been used for
168 geophysical studies because their phase transitions are good analogs for those of oxyspinel
169 compounds. These are known to show phase transitions in high-pressure regimes (e.g., 29
170 GPa for FeCr₂O₄; Shu et al., 2007), while thiospinel transitions occur at lower pressure (e.g.,
171 9 GPa for FeCr₂S₄; Amiel et al. 2011) (Manjon et al. 2014; Santamaría-Pérez et al. 2012).

172 It seems probable that additional occurrences of joegoldsteinite in enstatite
173 chondrites and IVA irons could be identified by making Mn x-ray maps of enstatite chondrite
174 thin sections and running EDS scans of sulfide grains in sections of iron meteorites. In
175 enstatite chondrites, joegoldsteinite is most likely to be found in association with other sulfide
176 phases; in IVA irons, it could be found as isolated crystals as in Social Circle or as parts of
177 polymineralic sulfide assemblages.

178

179

ACKNOWLEDGMENTS

180 We thank V. Tsurkan for providing a synthesized FeCr₂S₄ crystal that greatly
181 facilitated analysis of the new mineral by EPMA. We are grateful to F. T. Kyte and R.

182 Esposito for their patience and for technical support with the electron microprobe. We thank
183 K. D. McKeegan for useful suggestions about finding inclusions in iron meteorites. We also
184 thank J. T. Wasson for comments on the manuscript. Helpful reviews and suggestions were
185 provided by T. J. McCoy, K. Keil, P. R. Buseck and Associate Editor S. B. Simon. SEM and
186 EBSD analyses were carried out at the Caltech Analytical Facility at the Division of
187 Geological and Planetary Sciences, which is supported, in part, by grant NSF EAR-0318518
188 and the MRSEC Program of the NSF under DMR-0080065. This work was supported in
189 part by NASA grant NNX14AF39G (A. E. Rubin).

190

191

REFERENCES CITED

- 192 Amiel Y., Rozenberg G. K., Nissim N., Milner A., Pasternak M. P., Hanfland M., and Taylor
193 R. D. (2011) Intricate relationship between pressure-induced electronic and structural
194 transformations in FeCr₂S₄. *Physical Review B*, 84(9), 224114.
- 195 Bertinshaw, J., Ulrich, C., Günther, A., Schrettle, F., Wohlauser, M., Krohns, S. and
196 Deisenhofer, J. (2014). FeCr₂S₄ in magnetic fields: possible evidence for a multiferroic
197 ground state. *Scientific Reports*, 4, 6079.
- 198 Bouchard, R. J. (1967). Spinel to defect NiAs structure transformation. *Materials Research*
199 *Bulletin*, 2(4), 459–464.
- 200 Brearley, A. J., and Jones, R. H. (1998) Chondritic meteorites. In: *Planetary Materials* (ed.
201 Papike, J. J.), pp. 3-1 – 3-398., Mineralogical Society of America, Washington, D.C.
- 202 Breen J. P., Rubin A. E. and Wasson J. T. (2015) Shock effects in IIIE iron meteorites:
203 Implications for parent-body history. *Meteoritics & Planetary Science*, 50,
204 abstract#5083.
- 205 Britvin S. N., Bogdanova A. N., Boldyreva M. M. and Aksenova G. Y. (2008)
206 Rudashevskyite, the Fe-dominant analogue of sphalerite, a new mineral: Description
207 and crystal structure. *American Mineralogist*, 93, 902-909.
- 208 Buchwald, V. F. (1975). *Handbook of iron meteorites, their history, distribution, composition,*
209 *and structure.* Center for Meteorite Studies, Arizona State University.
- 210 Darcy, L., Baltzer, P. K., and Lopatin, E. (1968). Magnetic and Crystallographic Properties of
211 the System MnCr₂S₄–MnInCrS₄. *Journal of Applied Physics*, 39(2), 898-899.
- 212 Denis, J., Allain, Y., and Plumier, R. (1970). Magnetic behavior of MnCr₂S₄ in high
213 magnetic fields. *Journal of Applied Physics*, 41(3), 1091-1093.
- 214 Keil, K. (1968). Mineralogical and chemical relationships among enstatite chondrites. *Journal*
215 *of Geophysical Research*, 73(22), 6945-6976.

- 216 Keil, K. (2007) Occurrence and origin of keilite, $(\text{Fe}_{>0.5}\text{Mg}_{<0.5})\text{S}$, in enstatite chondrite
217 impact-melt rocks and impact-melt breccias. *Chemie der Erde*, 67, 37-54.
- 218 Lin, Y. T., Nagel, H-J., Lundberg, L. L., and El Goresy, A. (1991) MAC88136 – The first EL3
219 chondrite (abstract). *Lunar and Planetary Science*, 22, 811-812.
- 220 Lotgering, F. K. (1968). Spin canting in MnCr_2S_4 . *Journal of Physics and Chemistry of Solids*,
221 29(12), 2193–2197.
- 222 Ma, C., and Rossman, G.R. (2008) Barioperovskite, BaTiO_3 , a new mineral from the
223 Benitoite Mine, California. *American Mineralogist*, 93, 154-157.
- 224 Ma, C., and Rossman, G.R. (2009) Tistarite, Ti_2O_3 , a new refractory mineral from the Allende
225 meteorite. *American Mineralogist*, 94, 841-844.
- 226 Ma, C., Beckett, J. R., and Rossman, G. R. (2012a) Buseckite, $(\text{Fe,Zn,Mn})\text{S}$, a new mineral
227 from the Zakłodzie meteorite. *American Mineralogist*, 97, 1226-1233.
- 228 Ma, C., Beckett, J. R., and Rossman, G. R. (2012b) Browneite, MnS , a new sphalerite-group
229 mineral from the Zakłodzie meteorite. *American Mineralogist*, 97, 2056-2059.
- 230 Manjon, F. J., Tiginyanu, I. and Ursaki, V. (2014) Pressure-Induced Phase Transitions in
231 AB_2X_4 Chalcogenide Compounds, Springer Series in Materials Science, 189, Springer,
232 Berlin, 243 pp.
- 233 McCoy T. J., McKeown D. A., Buechele A. C., Tappero R. and Gardner-Vandy K. G. (2014)
234 Do enstatite chondrites record multiple oxidation states? *Lunar and Planetary Science*,
235 45, abstract#1983.
- 236 Menyuk, N., Dwight, K., and Wold, A. (1965) Magnetic properties of MnCr_2S_4 . *Journal of*
237 *Applied Physics*, 36(3), 1088-1089.
- 238 Moren A. E. and Goldstein J. I. (1978) Cooling rate variations of group IVA iron meteorites.
239 *Earth and Planetary Science Letters*, 40, 151-161.

- 240 Plumier, R. (1980) The magnetic structure of sulfur spinel MnCr_2S_4 under applied magnetic
241 field. *Journal of Physics and Chemistry of Solids*, 41(8), 871–873.
- 242 Raccach, P. M., Bouchard, R. J., and Wold, A. (1966) Crystallographic study of chromium
243 spinels. *Journal of Applied Physics*, 37, 1436-1437.
- 244 Rubin, A. E., and Keil, K. (1983) Mineralogy and petrology of the Abee enstatite chondrite
245 breccia and its dark inclusions. *Earth Planet. Sci. Lett.*, 62, 118-131.
- 246 Rubin, A. E., Zolensky, M. E., and Bodnar, R. J. (2002) The halite-bearing Zag and
247 Monahans (1998) meteorite breccias: Shock metamorphism, thermal metamorphism
248 and aqueous alteration on the H-chondrite parent body. *Meteorit. Planet. Sci.*, 37,
249 125-141.
- 250 Santamaría-Pérez, D., Amboage, M., Manjón, F. J., Errandonea, D., Muñoz, A.,
251 Rodríguez-Hernández, P., Mújica, A., Radescu, S., Ursaki, V. V., and Tiginyanu, I. M.
252 (2012) Crystal chemistry of CdIn_2S_4 , MgIn_2S_4 , and MnIn_2S_4 thiospinels under high
253 pressure. *Journal of Physical Chemistry C*, 116, 14078-14087.
- 254 Scott, E. R. D., Haack, H., and McCoy, T. J. (1996) Core crystallization and silicate-metal
255 mixing in the parent body of the IVA iron and stony-iron meteorites. *Geochimica et*
256 *Cosmochimica Acta*, 60, 1615-1631.
- 257 Shu J., Mao L., Hemley R. J., and Mao H. (2007) Pressure-induced distortive phase transition
258 in chromite-spinel at 29 GPa. *Materials Research Society Symposium Proceedings*,
259 987.
- 260 Tsurkan, V., Hemberger, J., Klemm, M., Klimm, S., Loidl, A., Horn, S. and Tidecks, R.
261 (2001) Ac susceptibility studies of ferrimagnetic FeCr_2S_4 single crystals. *Journal of*
262 *Applied Physics*, 90, 4639-4644
- 263 Tsurkan, V., Mücksch, M., Fritsch, V., Hemberger, J., Klemm, M., Klimm, S., Körner, S.,
264 Krug von Nidda, H.-A., Samusi, D., Scheidt, E.-W., Loidl, A., Horn, S. and Tidecks,

- 265 R. (2003). Magnetic, heat capacity, and conductivity studies of ferrimagnetic MnCr_2S_4
266 single crystals. *Physical Review B*, 68(13), 134434.
- 267 Vaqueiro, P., Powell, A. V., Hull, S., and Keen, D. A. (2001). Pressure-induced phase
268 transitions in chromium thiospinels. *Physical Review B*, 63(6), 064106.
- 269 Wasson, J. T., and Richardson, J. W. (2001). Fractionation trends among IVA iron
270 meteorites: contrasts with IIIAB trends. *Geochimica et Cosmochimica Acta*, 65(6),
271 951–970.
- 272 Wasson, J. T., Kallemeyn, G. W. and Rubin, A. E. (1994) Equilibration temperatures of EL
273 chondrites: A major downward revision in the ferrosilite contents of enstatite.
274 *Meteoritics*, 29, 658-661.
- 275 Weisberg, M. K. and Kimura, M. (2012) The unequilibrated enstatite chondrites. *Chemie der*
276 *Erde*, 72, 101-115.
- 277 Williams, C. V., Rubin, A. E., Keil, K., and San Miguel, A. (1985) Petrology of the Cangas
278 de Onis and Nulles regolith breccias: Implications for parent body history. *Meteoritics*,
279 20, 331-345.
- 280 Willis J. and Wasson J. T. (1978a) Cooling rates of Group IVA iron meteorites. *Earth and*
281 *Planetary Science Letters*, 40, 141-150.
- 282 Willis J. and Wasson J. T. (1978b) A core origin for Group IVA iron meteorites: A reply to
283 Moren and Goldstein. *Earth and Planetary Science Letters*, 40, 162-167.
- 284
- 285

286 Table 1. Analytical data for type specimen of joegoldsteinite.

Constituent	wt.%	Range	sd
S	44.3	43.6-44.7	0.35
Cr	36.2	35.7-36.5	0.32
Mn	15.8	15.4-16.0	0.21
Fe	4.5	4.2-5.2	0.30
Ni	0.09	0.02-0.13	0.04
Cu	0.08	0.05-0.11	0.02
Co	<0.03	---	---
total	101.0		

287

288 **Table 2. Calculated X-ray powder diffraction data for joegoldsteinite ($I_{\text{rel}} > 1$).**

<i>h</i>	<i>k</i>	<i>l</i>	<i>d</i> [Å]	<i>I</i> _{rel}
1	1	1	5.837	18
2	2	0	3.574	34
3	1	1	3.048	100
2	2	2	2.919	2
4	0	0	2.528	58
4	2	2	2.064	12
3	3	3	1.946	3
5	1	1	1.946	50
4	4	0	1.787	95
5	3	1	1.709	3
6	2	0	1.599	4
5	3	3	1.542	12
4	4	4	1.459	10
5	5	1	1.416	4
6	4	2	1.351	7
5	5	3	1.316	11
7	3	1	1.316	5

8	0	0	1.264	13
7	3	3	1.235	1
8	2	2	1.191	2
6	6	0	1.191	2
7	5	1	1.167	8
5	5	5	1.167	4
8	4	0	1.130	12
9	1	1	1.110	2
9	3	1	1.060	12
8	4	4	1.032	27
7	7	1	1.016	1
10	2	0	0.991	2
8	6	2	0.991	2
9	5	1	0.977	17
9	5	3	0.943	2
10	4	2	0.923	1
11	1	1	0.912	1
7	7	5	0.912	1
8	8	0	0.894	12

11	3	1	0.883	1
9	5	5	0.883	3
8	8	2	0.880	1
8	6	6	0.867	2
9	7	3	0.858	7
12	0	0	0.843	2
8	8	4	0.843	9
7	7	7	0.834	1
12	2	2	0.820	1
10	6	4	0.820	9
9	7	5	0.812	13
11	5	3	0.812	3
12	4	0	0.799	40

289

290

291

292

FIGURE CAPTIONS

293 Fig. 1. Backscattered electron (BSE) images showing two joegoldsteinite grains in Social
294 Circle thick section UCLA TK 724.

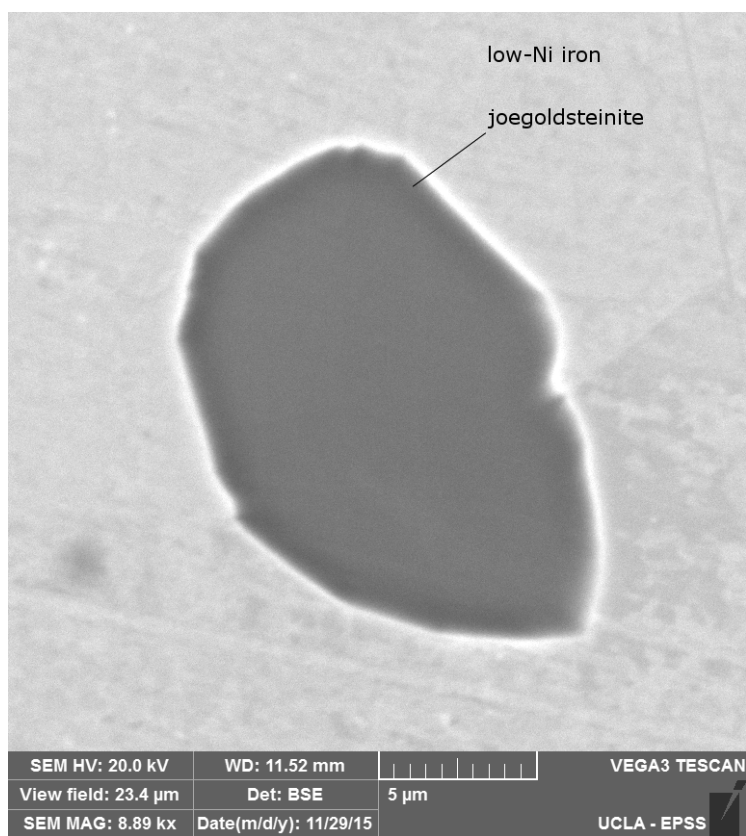
295 Fig. 2. BSE image showing the $(\text{Mn,Fe})\text{Cr}_2\text{S}_4$ phase in Caltech Indarch section ICM3.

296 Fig. 3. (left) EBSD patterns of the joegoldsteinite crystals in Figure 1, and (right) the patterns
297 indexed with the $Fd3m$ MnCr_2S_4 structure.

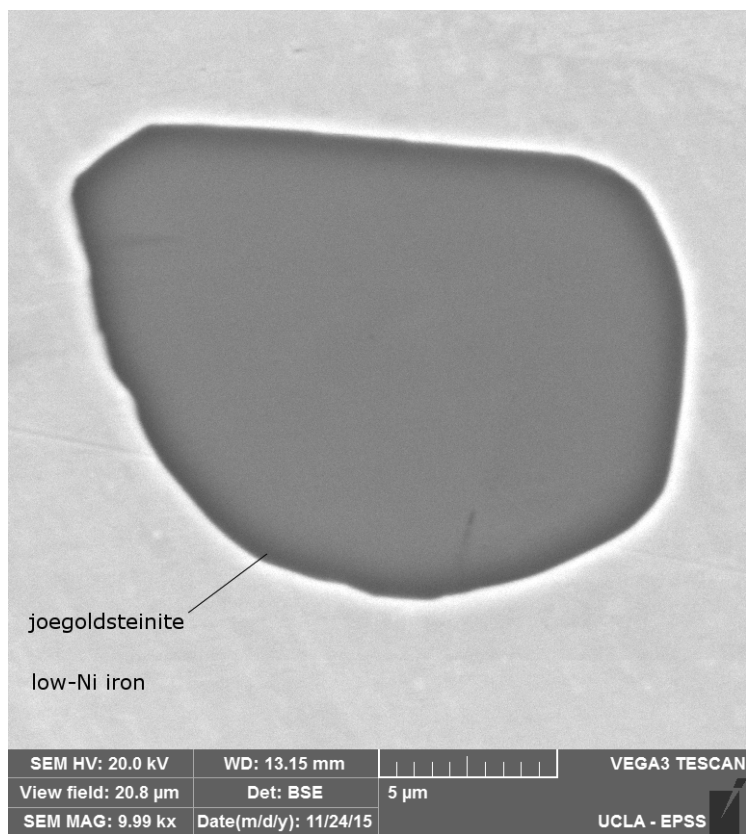
298

299

300



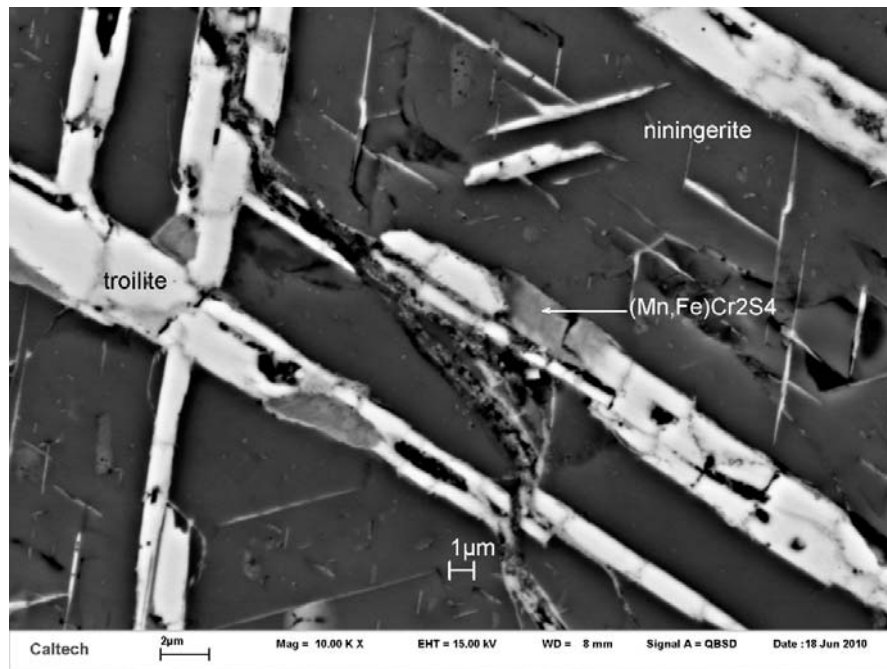
301



302 Fig. 1.

303

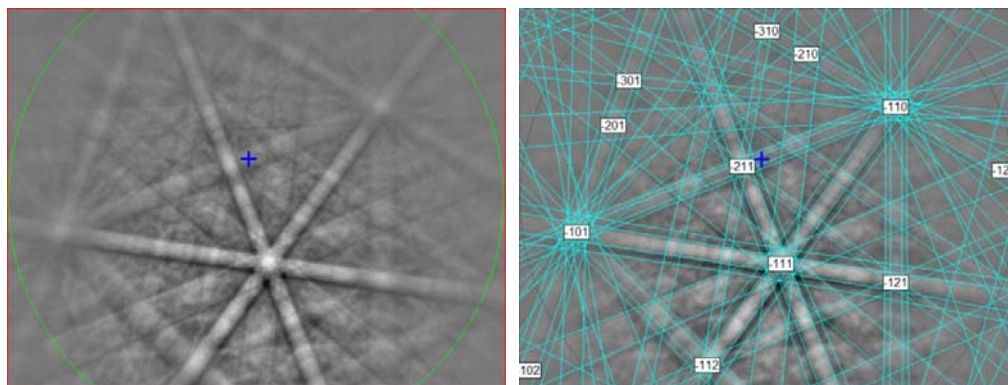
304



305

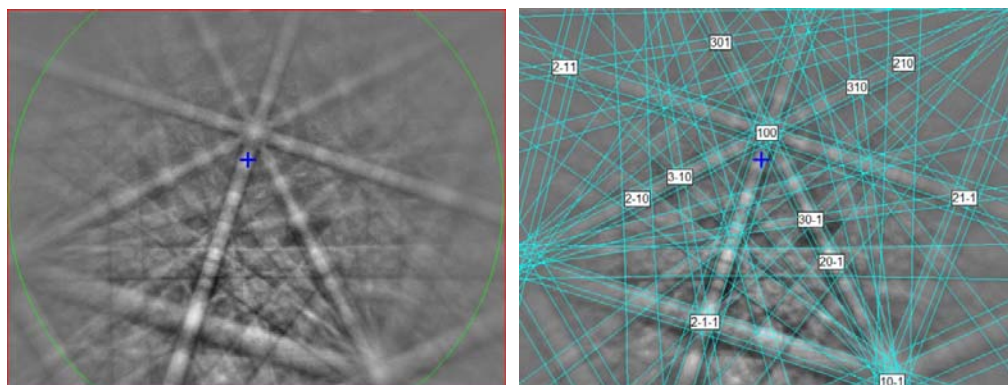
306 Fig. 2.

307



308

309



310

311 Fig. 3.

312